EXTENDED REPORT

Phosphatidylinositol 3-kinase delta pathway: a novel therapeutic target for Sjögren's syndrome

Saba Nayar ,[1] Joana Campos ,[1] Charlotte G Smith ,[1] Valentina Iannizzotto ,[1] David H Gardner ,[1] Serena Colafrancesco ,[1,2] Elena Pipi ,[1] Florian Kollert ,[1,3,4] Kelly J Hunter ,[5] Charlotte Brewer ,[5] Christopher Dominic Buckley ,[6] Simon J Bowman ,[1] Roberta Priori ,[2] Guido Valesini ,[2] Maria Juarez ,[7] William A Fahy ,[7] Benjamin A Fisher ,[6] Andrew Payne ,[7] Rodger A Allen ,[7] Francesca Barone [1,3]

Handling editor Josef S Smolen

► Additional material is published online only. To view please visit the journal online (http://dx.doi.org/10.1136/annrheumdis-2017-212619).

For numbered affiliations see end of article.

Correspondence to
Francesca Barone, Centre for Translational Inflammation Research, Institute of Inflammation and Ageing College of Medical & Dental Sciences, University of Birmingham Research Laboratories, Queen Elizabeth Hospital, Birmingham B15 2WB, UK; f.barone@bham.ac.uk

Received 30 October 2017
Revised 28 September 2018
Accepted 18 October 2018

To cite: Nayar S, Campos J, Smith CG, *et al*. *Ann Rheum Dis* Epub ahead of print: [*please include* Day Month Year]. doi:10.1136/annrheumdis-2017-212619

ABSTRACT

Background The phosphatidylinositol 3-kinase delta isoform (PI3Kδ) belongs to an intracellular lipid kinase family that regulate lymphocyte metabolism, survival, proliferation, apoptosis and migration and has been successfully targeted in B-cell malignancies. Primary Sjögren's syndrome (pSS) is a chronic immune-mediated inflammatory disease characterised by exocrine gland lymphocytic infiltration and B-cell hyperactivation which results in systemic manifestations, autoantibody production and loss of glandular function. Given the central role of B cells in pSS pathogenesis, we investigated PI3Kδ pathway activation in pSS and the functional consequences of blocking PI3Kδ in a murine model of focal sialoadenitis that mimics some features of pSS.

Methods and results Target validation assays showed significant expression of phosphorylated ribosomal protein S6 (pS6), a downstream mediator of the phosphatidylinositol 3-kinase delta (PI3Kδ) pathway, within pSS salivary glands. pS6 distribution was found to co-localise with T/B cell markers within pSS aggregates and the CD138+ plasma cells infiltrating the glands. In vivo blockade of PI3Kδ activity with seletalisib, a PI3Kδ-selective inhibitor, in a murine model of focal sialoadenitis decreased accumulation of lymphocytes and plasma cells within the glands of treated mice in the prophylactic and therapeutic regimes. Additionally, production of lymphoid chemokines and cytokines associated with ectopic lymphoneogenesis and, remarkably, saliva flow and autoantibody production, were significantly affected by treatment with seletalisib.

Conclusion These data demonstrate activation of PI3Kδ pathway within the glands of patients with pSS and its contribution to disease pathogenesis in a model of disease, supporting the exploration of the therapeutic potential of PI3Kδ pathway inhibition in this condition.

Key messages

What is already known about this subject?
► The phosphatidylinositol 3–kinase pathway is involved in the pathogenesis of proliferative disorders and autoimmunity.

What does this study add?
► Our study demonstrate that this pathway is active in SS and that pharmacological targetting of this pathway drives disease amelioration in an animal model of sialoadenitis that recapitulates some feayures of SS.

How might this impact on clinical practice or future developments?
► This proof of concept study support future development of therapeutics against PI3KD in SS.

INTRODUCTION

The phosphatidylinositol 3-kinase delta isoform (PI3Kδ) belongs to the class 1 phosphoinositide-3-kinase family of intracellular lipid kinases that regulate metabolism, survival, proliferation, apoptosis, growth and cell migration.[1] Extensive data demonstrate a central role for PI3K signalling in several aspects of adaptive immune responses. Expression of the catalytic subunit of PI3Kδ is greatly enriched in lymphocytes. In B cells, PI3Kδ represents the predominant PI3K isoform to transduce signals derived from the B cell receptor and receptors binding B cell survival factors, cytokines, chemokines and costimulatory molecules.[2–4] Downstream signalling on PI3Kδ activation results in the activation of AKT and mTOR; the latter exists in two major protein complexes, the rapamycin-sensitive mTORC1 (in complex with raptor) and the rapamycin-insensitive mTORC2 (in complex with rictor). A key substrate of mTORC1, ribosomal protein S6 kinase (S6K), phosphorylates ribosomal protein S6 (pS6), which can thereby act as a marker of active PI3K-mTOR signalling. The sensitivity of pS6 expression to PI3Kδ signalling has been demonstrated in both T and B cells.[5 6]

The significant role of PI3Kδ in regulating B cell biology has led to the development of PI3Kδ inhibitors as therapeutics for B cell malignancies.[7–9] Idelalisib, a PI3Kδ selective inhibitor, has recently received Food and Drug Administration approval for the treatment of chronic lymphocytic leukaemia and non-Hodgkin's lymphoma (NHL). Clinical trials have demonstrated the ability of idelalisib to inhibit B cell survival and interfere with microenvironment-derived signals responsible for maintenance of malignant cells within the lymph node.[7] The established role of PI3Kδ in B cell hyperactivity suggest that this pathway is an attractive target for

autoimmune conditions characterised by B cell hyperactivation, such as primary Sjögren's syndrome (pSS).

pSS is characterised by systemic autoantibody production and local, predominantly B cell infiltration of the exocrine glands that often results in functional loss. Cellular infiltrates are characterised by ectopic production of lymphoid chemokines, T/B cell segregation and formation of follicular dendritic cell networks within ectopic germinal centres (GC).[10 11] Moreover, local expression of *AICDA*, the gene encoding for the activation-induced cytidine deaminase (AID), the enzyme instrumental for B cell affinity maturation, is expressed in pSS GC where it is believed to support local autoantibody production.[12] Progressive enlargement of pSS inflammatory foci is characterised by increased accumulation of activated B cells, and in some cases, local emergence of post-GC malignant clones responsible for the development of NHL.[13–18] Dysregulated B cell activation, locally manifested by salivary gland swelling and production of anti-SSA and anti-SSB autoantibodies, is also accompanied by systemic increases in immunoglobulins and autoantibodies, including rheumatoid factor and cryoglobulins.[19–24] Additional systemic features associated with B cell hyperactivity, such as lymphadenopathy, night sweats and loss of weight are often observed during lymphoma development.[21 24 25] The dysfunctional humoral response present in these patients supports the investigation of PI3Kδ in pSS pathogenesis and its blockade as a therapeutic option for this condition.

MATERIALS AND METHODS

Mice and salivary gland cannulation

C57BL/6 mice were purchased from Charles River and were maintained under specific pathogen-free conditions in the Biomedical Service Unit at the University of Birmingham according to Home Office and local ethics committee regulations. Under ketamine/domitor anaesthesia, the submandibular glands of female C57BL/6 (8–12 weeks) were intraductally cannulated with 10^8–10^9 plaque-forming unit (pfu) of luciferase-encoding replication-defective adenovirus (AdV5), as previously described.[26] Mice were sacrificed at day 15 post-cannulation (pc) (peak of organisation of the lymphoid aggregates). To collect samples, mice were given general anaesthesia as mentioned above and were then secured in the supine position. Salivation was induced by subcutaneous administration of 10 mg/kg pilocarpine (Sigma-Aldrich) in phosphate buffered saline (PBS). Saliva was collected with a pipet over a 10 min period and transferred into weighed eppendorf tubes, the tubes were then reweighed and the volume of saliva calculated (1 mg=1 µL saliva). Results were expressed as mg saliva/10 min/g body weight.

Seletalisib inhibitor

The in vitro and in vivo properties of seletalisib have been described previously.[27] Mice were gavaged at a dose of 10 mg/kg with seletalisib every day starting from day 0, day 3, day 5 and day 8 pc.

Human salivary gland biopsies from patients with pSS

Minor salivary gland (mSGs) samples were obtained from the Human Biomaterials Resource Centre at the University of Birmingham under ethics number 10-018 and from the Sjögren's cohort at the University of Rome, Sapienza under ethics Harmonics H2020. Specimens were identified among samples obtained by patients diagnosed with pSS according to the 2002 American European Consensus Group Criteria criteria[28] and fulfilling the histological criteria for the diagnosis of pSS (presence of aggregates>1 focus score). All patients included were untreated with immunosuppressive drugs including steroids.

Non-specific sialoadenitis samples were selected among patients undergone investigation for pSS, because of clinical symptoms of dryness (eyes and/or mouth) but either did not fulfil the classification criteria for pSS and/or were not clinically diagnosed as primary or secondary SS by the leading physician table 1.

On patients collected between 2012 and 2018, EULAR Sjögren's Syndrome Disease Activity Index (ESSDAI) data were available and reported in table 1.

Table 1 Baseline characteristics of subjects included in the study

Cohorts 1 and 2 Birmingham		
Baseline characteristics	**pSS (cohort 1)**	**Sicca (cohort 1)**
Age (years)*	63.0 (55, 67)	47 (46, 52)
Female†	9/9 (100)	3/3 (100)
Anti-Ro antibody positive†	7/9 (78)	0/0 (0)
Anti-La antibody positive†	6/9 (67)	0/0 (0)
IgG (g/L)*	17.6 (12.9, 42.5)	–
Focus score	>1	N/A
Germinal centre†	–	N/A
ESSDAI	–	–
N/A, non applicable.		
Baseline characteristic	**pSS (cohort 2)**	**Sicca (cohort 2)**
Age (years)*	56.0 (24, 57)	41 (32, 76)
Female†	4/5 (80)	3/5 (60)
Anti-Ro antibody positive†	4/5 (80)	0/0 (0)
Anti-La antibody positive†	2/5 (40)	0/0 (0)
IgG (g/L)*	13.05 (9.95, 19.94)	9.26 (7.51, 13.98)
Focus score*	1.29 (0.8, 2.14)	N/A
Germinal centre†	2/4 (50)	N/A
ESSDAI	9 (8, 17)	N/A
Cohort 3. Rome		
Baseline characteristic	**pSS**	**Sicca**
Age (years)*	48 (26,72)	55 (37,70)
Female†	15/17 (88.2)	15/15 (100)
Anti-Ro antibody positive†	11/17 (64.7)	0/0 (100)
Anti-La antibody positive†	8/17 (47.1)	0/0 (100)
Anti-nuclear antibody positive†	12/17 (70.6)	0/0 (100)
Hyperglobulinemia†	7/17 (41.2)	0/0 (100)
Focus score*	2.8 (1,10)	N/A
Germinal centre†	11/17 (64.7)	N/A
ESSDAI*	1 (0, 7)	0 (0, 2)

*Median (range).
†Number positive (%).
BAFF, B cell activating factor; ESSDAI, EULAR Sjögren's Syndrome Disease Activity Index; Ig, immunoglobulin; pSS, primary Sjögren's syndrome.

Histology and immunofluorescence

Immunofluorescence (IF) staining was performed as previously described on formalin-fixed, paraffin-embedded (FFPE) labial salivary gland biopsies from patients with SS[10 29 30] and on murine SGs obtained from virus cannulated and control mice.[30]

The following antibodies were used: for mouse CD45 clone 30-F11, CD19 clone eBio1D3 and CD3e clone ebio500A2 (from eBiosciences) and for humans CD3 polyclonal rabbit or monoclonal mouse (Dako), CD20 clone L26 (Dako), CD138

and CD68 (Abd Serotech) and pS6 polyclonal rabbit (Cell signalling).

RNAScope

IF staining was performed as previously described on FFPE labial salivary gland biopsies from patients with SS.[10 29 30] Samples were probed for PI3KCD ref.520988 (ACDBio) following manufacturer's instructions (ACDBio). Samples were double stained with antihuman CD45 NCL-L-LCA (Leica).

Enzymatic digestion and isolation of cells

ADV5 infected SGs from seletalisib-treated and vehicle-treated mice were isolated from culled animals at different time points. Glands were dissected and placed in 1 mL of RPMI-1640 (with 2% fetal calf serum (FCS)) on ice. Once all SGs were collected, RPMI-1640 was removed, replaced with 2 mL enzyme mix (RPMI with 2% FCS, 0.8 mg/mL dispase, 0.2 mg/mL collagenase P and 0.1 mg/mL DNase I) and digested as previously described.[31]

Flow cytometry analysis and sorting

Single cell suspensions were incubated with 100 µL diluted antibodies for 30 min at 4°C in ice-cold fluorescence-activated cell sorting (FACS) buffer (0.5% bovine serum albumin, 2 mM EDTA in PBS) with 'cocktails' of the following antibodies: CD45 clone 30-F11, CD3e clone 145–2 C11, CD4 clone RM4-5, CD62L clone MEL-14, CD44 clone IM7, CD8a clone 53–6.7, B220 clone RA3-6B2, CD23 clone B3B4, CD19 clone 1D3 and CD5 clone 53–7.3 (all from eBiosciences), CD21 clone 7G6 (BD biosciences) and CD11c clone N418, F4/80 clone BM8, CD64 clone X54-5/7.1 and NK1.1 clone PK136. Intracellular staining for Ki67 clone B56 (BD Biosciences) and pS6 PE and pAKT Alexa Fluor 488 (Cell signalling) was performed by using the Cytofix/Perm kit (BD biosciences) and Fixation/Permeabilization Buffer set (ebiosciences) according to the manufacturer's protocol. Cells were resuspended in FACS buffer and then analysed using a Cyan-ADP (Dako) or Fortessa (BD) with forward/side scatter gates set to exclude non-viable cells. Cells of interest were sorted by using BD FACSAria. Data were analysed with FlowJo software (Tree Star).

Microdissection, mRNA isolation, qRT-PCR

Microdissection and laser catapulting were performed on Cresyl-violet (0.1% in ethanol)-stained frozen tissue sections from salivary gland samples and tonsil GCs as previously described.[32]

Total RNA was isolated either from murine and human SGs with an RNeasy mini kit (Qiagen), from microdissected tissue or from sorted cells. RNA was then reverse transcribed using the high capacity reverse transcription cDNA synthesis kit (Applied Biosystems) according to the manufacturer's specifications. Reverse transcription was carried out on a Techne 312 Thermal Cycler PCR machine. Quantitative real-time (qRT)-PCR (Applied Biosystems) was performed on cDNA samples for *ccl19*, *cxcl13*, *lta*, *ltb* and *baff* mRNA expression. β-actin and pdgfrβ were used as an endogenous control. The primers and probes used were from Applied Biosystems (table 2). qRT-PCR was run in duplicates on a 384-well PCR plate (Applied Biosystems) and detected using an ABI PRISM 7900HT instrument. Results were analysed with the Applied Biosystems SDS software (SDS V.2.3) as previously described.[30]

Table 2 Primers and probes used for quantitative PCR

Gene	Assay ID
Mouse β-actin	Mm01205647_g1
Mouse Pdgfrβ	Mm00435546_m1
Mouse AICDA	Mm00507774_m1
Mouse BAFF	Mm00840578_g1
Mouse CXCL13	Mm00444533_m1
Mouse CXCR5	Mm00432086_m1
Mouse CCL19	Mm00839967_g1
Mouse CCR7	Mm01301785_m1
Mouse CXCL12	Mm00445553_m1
Mouse CXCR4	Mm01292123_m1
Mouse LTβ	Mm00484254_m1
Mouse LTα	Mm00484254_m1
Mouse IL-23	Mm00484254_m1
Mouse IL-6	Mm00434256_m1
Mouse IFNγ	Mm00434774_g1
Mouse TNFα	Mm00443258_m1
Mouse IL-1β	Mm00434228_m1

Lipid analysis

Salivary gland tissue was pulverised in liquid nitrogen using a mortar and pestle and determination of phosphatidylinositol (3,4,5)-trisphosphate (PIP3) levels, including lipid extraction, derivatisation and mass spectrometric analysis, was carried out as described previously.[33]

RESULTS

Target validation of PI3Kδ pathway engagement in SGs of patient with pSS

We confirmed the expression of PI3KCD transcript mRNA name for PI3Kδ in sorted peripheral blood mononuclear cell from patients with pSS (figure 1A) and in total mRNA isolated from minor SGs from pSS and sicca controls (figure 1B). Transcript levels of PI3KCD significantly correlated with the focus score (FSC) calculated in the same SGs (figure 1C) and associate with immune activation markers such as the presence of autoantibodies, hyperglobulinaemia and the presence of GCs (online supplementary figure 1). qRT-PCR on microdissected tissue and RNAScope confirmed localisation of the transcript for PI3Kδ within the foci and in particular within GC+foci (figure 1D,E and control tonsil in the online supplementary figure 1).

In order to assess activation of the PI3Kδ pathway in minor SG biopsies and confirm its local engagement, we used IF to detect the presence of the phosphorylated ribosomal protein S6 (pS6),[27 34] in pSS and non-specific sialoadenitis control (NSCS) tissue. Significant expression of pS6 was observed in salivary gland biopsies of patients with pSS as compared with non-specific sialoadenitis. In NSCS, pS6 staining was only detected within the epithelium and not present in all samples analysed (figure 1F). On the contrary, in pSS, intense pS6 staining was detected within the lymphoid aggregates and on the periphery of the foci, in co-localisation with T (CD3+) and B (CD20+) cells and myeloid cells (figure 1G,H and online supplementary figure 1 for pSS and tonsil GC, used as control). This correlated with the extent of infiltration of the glands (online supplementary figure 1).

Interestingly, intense pS6 staining was detected in co-localization with CD138+ plasma cells in pSS SGs as demonstrated by IF and flow cytometry (figure 1H,I). pS6 positive

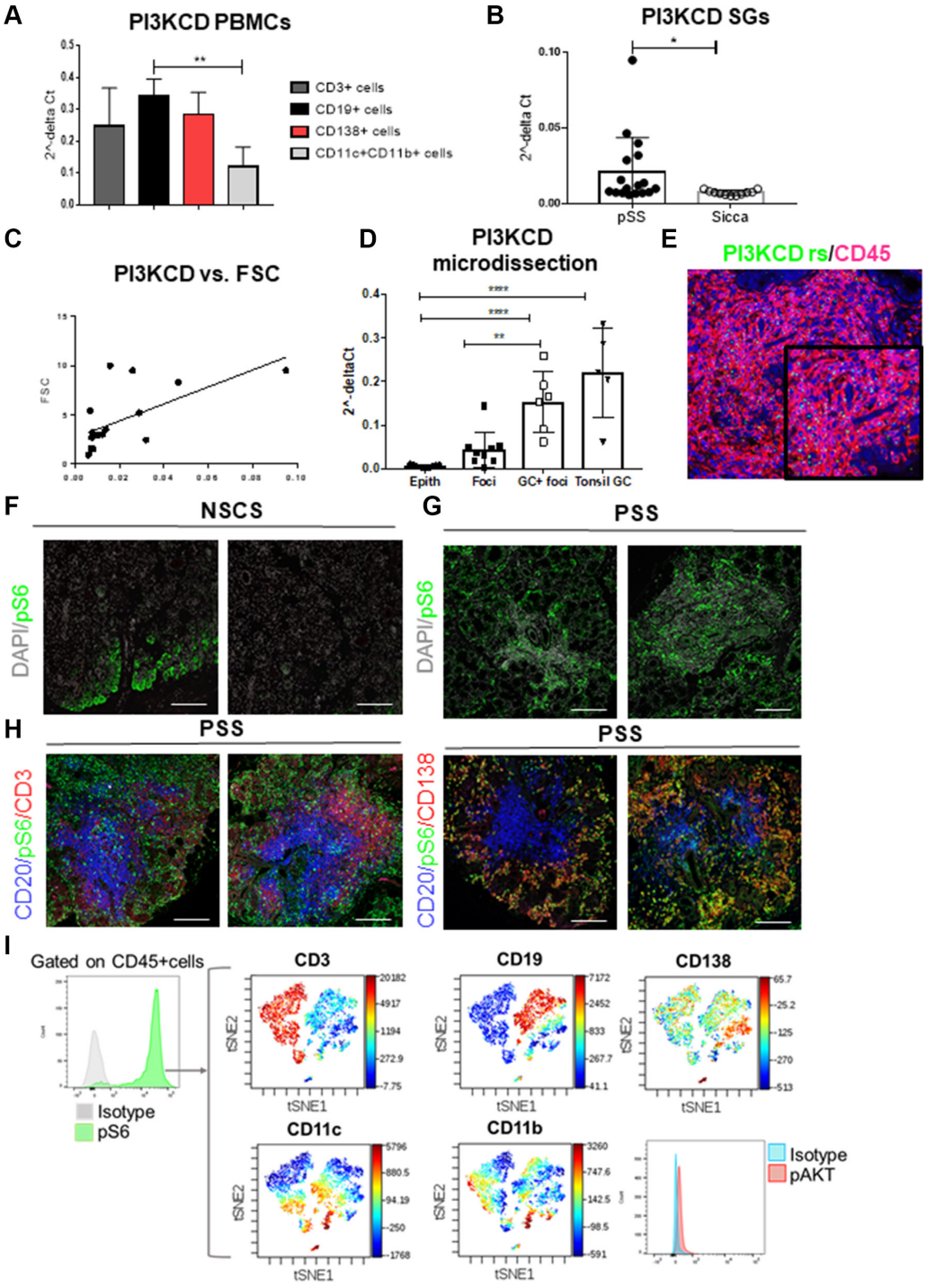

Figure 1 (A) Quantitative real-time (qRT)-PCR analysis of PI3KCD transcripts in peripheral blood mononuclear cell (PBMC) isolated from patients with primary Sjögren's syndrome (pSS). CD3+ cells (dark grey bar), CD19+ cells (black bar), CD138+ cells (red bar), CD11c+CD11b+ cells (light grey bar). Results represented as mean±SD of five patients; **p<0.01, one-way analysis of variance (ANOVA). (B) qRT-PCR analysis of PI3KCD transcripts in total mRNA isolated from salivary glands of patients with pSS (black circles) and sicca controls (open circles). Results represented as mean±SD of 15–17 patients in each group; *p<0.05, unpaired t-test. (C) Correlation between focus scores (FSC) and levels of PI3KDC expressed as 2^-DCT detected in frozen salivary galnds from patients with pSS. R^2 0.3941, p=0.0092. (D) qRT-PCR analysis of PI3KCD transcripts in microdissected epithelium, foci, germinal centre positive (GC+) foci from salivary glands of patients with pSS and GCs isolated from tonsils. Results represented as mean±SD of 5–10 biological replicates in each category; **p<0.01, ****p<0.0001, one-way ANOVA. (E) Microphotograph of minor salivary glands from patients with pSS, showing in red CD45 staining and in green PI3KCD RNA (visualised with RNAScope). (F) Representative microphotograph of salivary glands from non-specific sialoadenitis control (NSCS) patients stained for the PI3Kδ pathway activation marker phosphorylated ribosomal protein S6 (pS6; green) and 4′,6-diamidino-2-phenylindole (DAPI; grey); scale bars=100 µm. (G) Representative microphotograph of salivary glands from patients with pSS with pS6 (green) and DAPI (grey). (H) Representative microphotographs showing pS6 (green) expression within CD20 (blue) and CD3 or CD138 (red) cells in salivary glands from patients with pSS; scale bars=100 µm. (I) Representative histogram showing flow cytometry staining for pS6 (green) and isotype control (grey) in CD45+ cells present in salivary glands of patients with pSS. viSNE plots of flow cytometry of pSS salivary gland CD45+pS6+ cells. Colours indicate cell expression level of labelled marker. Histogram showing pAkt expression in CD45+pS6+ cells.

cells encompassed also T, B and dendritic cells (DCs) and AKT activation (figure 1I).

These data suggest that PI3Kδ is engaged in several cell types within pSS inflammatory infiltrates and might be involved in the perpetuation of the local autoimmune response.

Blockade of PI3Kδ pathway reverses lymphocytic infiltration in a mouse model of focal sialoadenitis

The in vivo functional role and downstream effect of PI3Kδ inhibition in pSS was tested taking advantage of a mouse model of focal sialoadenitis induced by direct delivery of a replication-deficient ADV5 within murine wild-type SGs.[26] Localised viral infection in this model mimics features of pSS, including the formation of focal lymphocytic aggregates, expression of lymphoid chemokines and cytokines as well as antinuclear antibodies.[26] First, expression of PI3KCD was confirmed in the CD45+ compartment of cannulated SGs from mice sacrificed at day 15 pc (figure 2A). Engagement of the pathway was confirmed by upregulation of pS6 and pAKT on isolated CD45+ cells, with a predominant expression in DCs, T cells, B cells and plasma cells (figure 2B–D). The large predominance of pS6+ DC in our model is probably related to the viral nature of the stimulus and is not reflecting entirely human pSS where the percentage of pS6+ cells only accounted for a minority of the CD11c+ and CD11b+ cells. Treatment of mice with seletalisib resulted in a significant decrease in the ratio between PIP3 and phosphatidylinositol (4,5)-biphosphate (PIP2), which demonstrated blockade of the PI3Kδ pathway (figure 2E). Moreover, seletalisib treatment induced downregulation of S6 phosphorylation in CD45+ cells isolated from infected SGs in treated mice but not in vehicle controls (figure 2F). Together, these data confirmed the activation of the PI3Kδ pathway in our model and the ability to modulate it by using seletalisib. ADV5 infected mice treated with seletalisib, either prophylactically (day 0 pc) or therapeutically (at day 3, 5 or 8 pc) showed a reduction in the absolute number of CD45+ cells in active treatment groups as compared with the vehicle-treated mice. This significant decrease was maintained in a full therapeutic regime when mice were treated from either day 3 or 5 pc (figure 3A). Although this significant reduction in CD45+ cell counts was not maintained when treated day 8 pc, a significant reduction was observed in specific immune cell populations, notably T and B cells (online supplementary figure 2). Together, these data confirm the therapeutic potential of this drug in established disease. Flow cytometry analysis revealed a marked reduction in absolute numbers of CD3+ T cells (both CD4 and CD8 cells) (figure 3B–D) as well as CD19+ B cells in all active treatment groups relative to controls (figure 3E). Within the overall T cell population, memory and effector CD4 and CD8+ cells were both affected (online supplementary figure 3). Moreover, all subsets of B cells (B1A, B1b, B1c, B2, marginal zone and follicular B cells) displayed marked decreases in absolute cell numbers (figure 3F–G and online supplementary figure 4). In addition, the proliferative ability of both T and B lymphocytes was impaired as demonstrated by a significant decrease in Ki67 staining in both the T and B compartment (figure 3H–I).

Following our observation of PI3Kδ activation in CD138+ plasma cells, we also explored the effect of seletalisib on this cell type in cannulated mice treated either with the compound or its vehicle. Inhibition of PI3Kδ resulted in a significant decline in the number of CD138+ plasma cells in all treatment groups, suggesting that the PI3Kδ pathway also regulates plasma cell homeostasis (figure 3J).

Interestingly, the effects observed on specific subpopulations can be different depending on the treatment regime used. While we did not observe a selective effect in samples treated prophylactically or from day 3 pc, we have observed a significant effect on all B cells as percentages (as well as absolute numbers) and in particular on B1a and MZ B cells in animals treated from day 5 pc (online supplementary figures 4 and 5).

Aggregate formation during salivary gland inflammation is abrogated in mice treated with seletalisib

Having observed a reduction in lymphocyte accumulation within SGs following seletalisib by flow cytometry, we wanted to confirm these observations by IF staining for CD3+ and CD19+ cells as well as to visualise any impact on the organisation of infiltrating lymphocytes. These data revealed impaired lymphoid aggregate formation in seletalisib-treated mice compared with those treated with vehicle. It was particularly marked in mice treated prophylactically with seletalisib, in which no visible lymphoid aggregate formation was evident. This was confirmed by quantification of the FSC, foci size and aggregate organisation, with all parameters demonstrating a significant reduction in the treated animals at day 15 pc as compared with the controls (figure 4A–C). Importantly, the abrogation of lymphocytic foci formation and organisation coincided with a decrease in antinuclear autoantibody production in mice treated with the PI3kδ inhibitor compound as compared with vehicle controls (figure 4 and online supplementary figure 4). Analysis of stimulated salivary flow also showed a significant improvement in saliva production in seletalisib-treated mice (figure 4E).

Inhibition of PI3Kδ pathway impairs the expression of ectopic lymphoneogenesis associated cytokines and chemokines

The reduced lymphocyte aggregation following seletalisib treatment led us to investigate its impact on the expression of factors that drive ectopic lymphoneogenesis. In accordance with the histological findings, qRT-PCR performed on whole SG tissue demonstrated significantly reduced transcript levels for the lymphoid cytokines (LTβ and LTα) in mice treated with seletalisib as compared with controls. Moreover, a significant reduction in CXCL13 and CXCL12 transcript levels was observed in seletalisib-treated mice, while a modest effect was observed for CCL19, one of the chemokines responsible for T cell migration within the affected glands. To further support the lymphoid chemokine expression and aggregate histological data, qRT-PCR analysis for CXCR5, CCR7 and CXCR4 mRNA also showed significantly lower transcript levels in seletalisib-treated mice when compared with vehicle controls. A significant reduction in B cell activating factor (BAFF) expression across all treatment groups tested as compared with vehicle-treated mice was also detected. Furthermore, marked suppression in AICDA mRNA transcripts (the gene encoding for AID) was observed in mice treated with PI3Kδ inhibitor (figure 5A).

IF analysis demonstrated decreased protein expression for CXCL13 and CCL21 in the mice analysed (figure 5B).

Overall, these results suggest that inhibition of the PI3Kδ pathway disrupts the positive feedback loop of lymphocytic infiltration and lymphoid chemokine production which is required for the establishment of ectopic GC and plasma cell survival niches in the affected SGs.

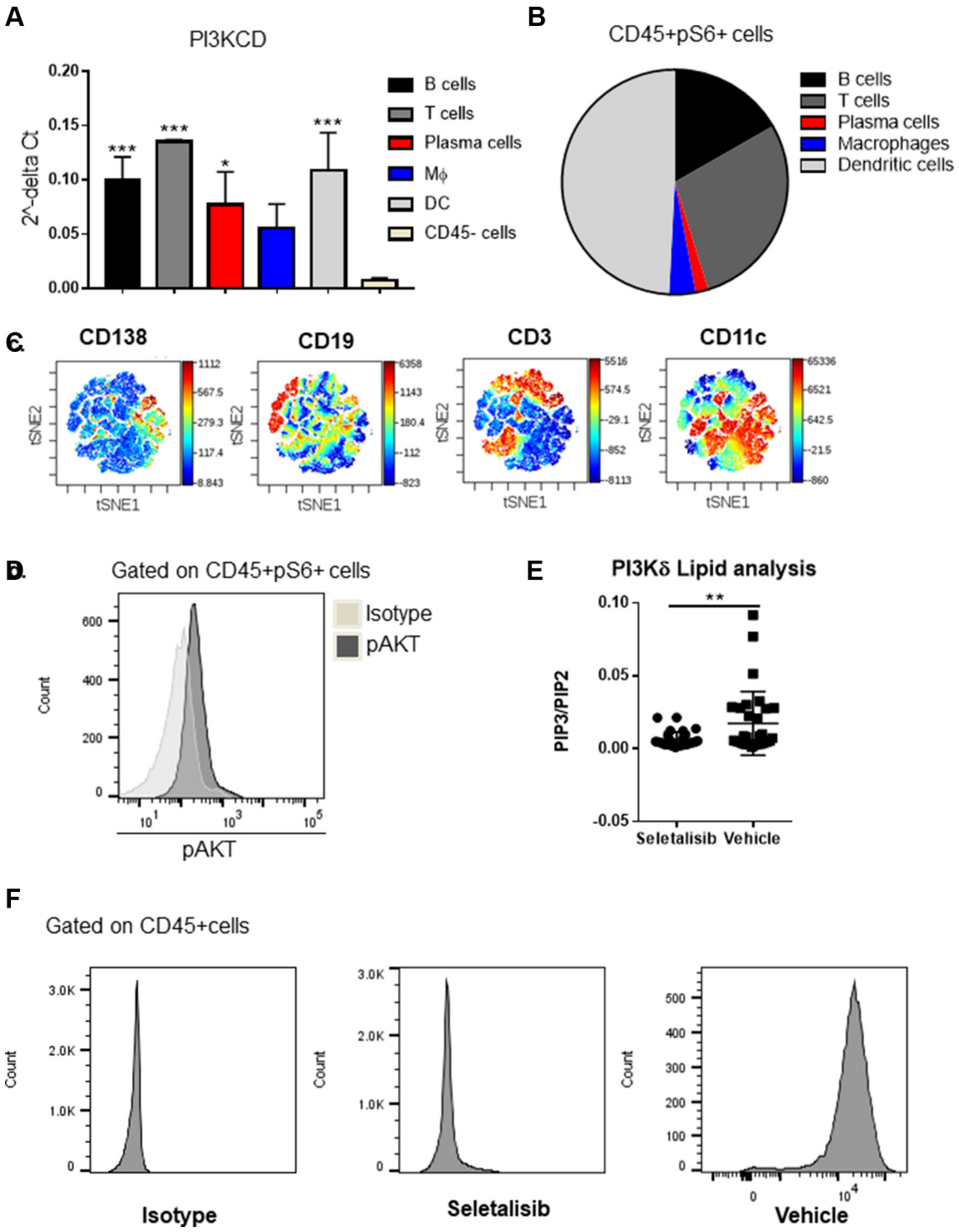

Figure 2 (A) Quantitative real-time PCR analysis of PI3KCD transcripts isolated cells from salivary glands of cannulated mice at day 15 postcannulation (pc). B cells (black bar), T cells (dark grey bar), plasma cells (red bar), macrophages (blue) and dendritic cells (light grey bar), CD45– cells (light yellow bars). Results represented as mean±SD from five mice; *p<0.5, ***p<0.001, one-way analysis of variance. (B) Pie chart showing distribution of different leucocyte populations within CD45+ phosphorylated ribosomal protein S6 (pS6+) cells present in salivary glands of wild-type (WT) mice at day 15 pc (C) viSNE plots of flow cytometry of day 15 pc salivary gland CD45+pS6+ cells. Colour indicates cell expression level of labelled marker. Data is representative of two independent experiments with five mice. (D) Histogram showing phosphorylation of Akt in CD45+pS6+ cells in salivary glands of WT mice at day 15 pc. (E) Graphs showing phosphatidylinositol (3,4,5)-trisphosphate (PIP3)/phosphatidylinositol (4,5)-biphosphate (PIP2) ratio in salivary glands of mice treated with seletalisib versus vehicle control to demonstrate effect of the compound directly in the salivary glands. Results represented as mean±SD of three independent experiments with five mice per group; **p<0.01, unpaired t-test. (F) Histogram showing pS6 expression levels within the CD45+ cells in day 15 pc salivary glands of mice treated with seletalisib as compared with the vehicle-treated mice. Isotype control also shown. The mice were treated with seletalisib or vehicle from day 12 pc onwards. Data is representative of experiments with three mice in each group.

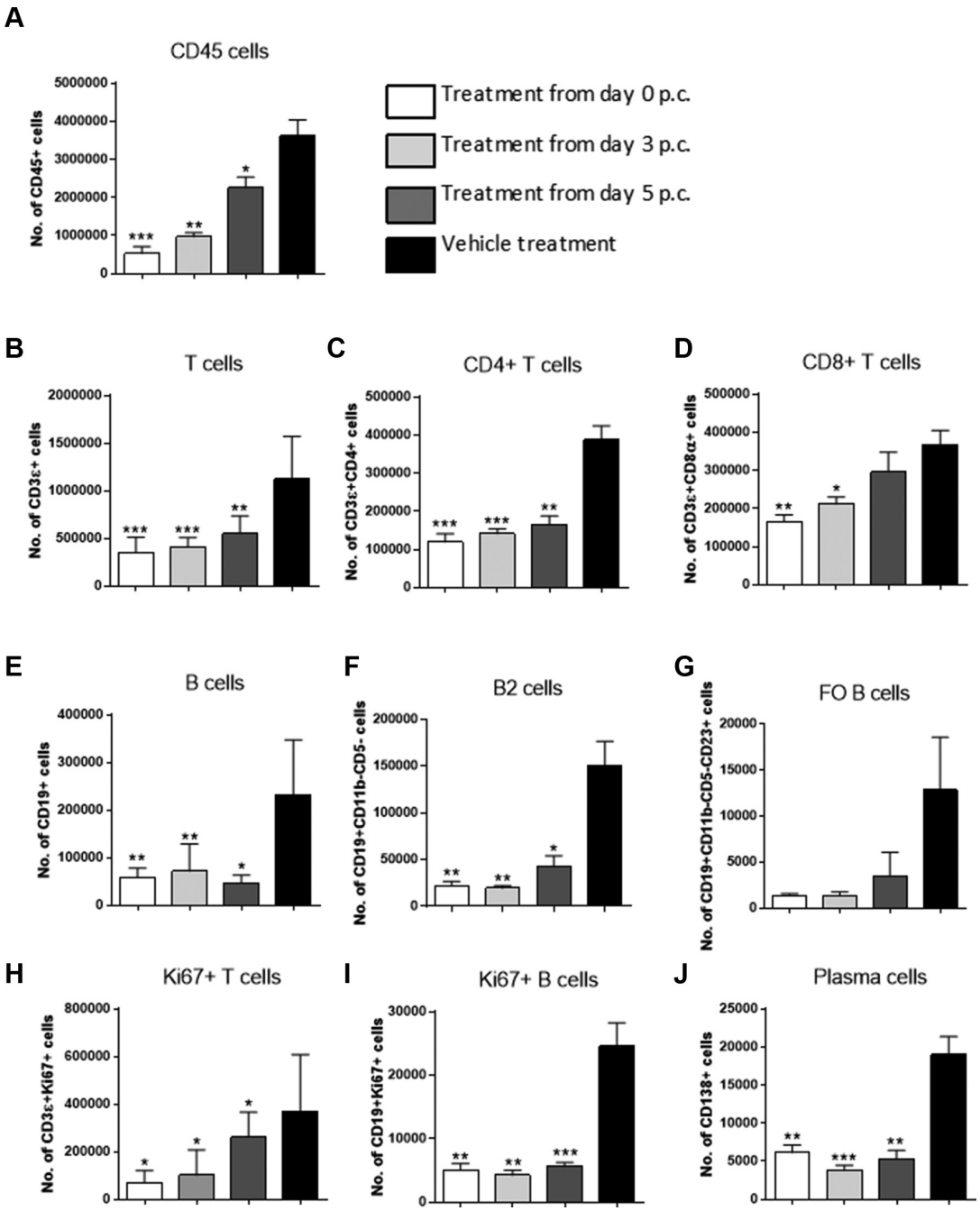

Figure 3 (A) Graphs summarising flow cytometry data for absolute numbers of CD45 cells in salivary glands of wild-type (WT) mice at day 15 postcannulation (pc) treated with seletalisib at day 0 (white bars), day 3 (light grey) and day 5 (dark grey) pc as compared with vehicle controls (black bars). Results represented as mean±SD of two independent experiments with five mice per group; *p<0.05, **p<0.01, ***p<0.001, one-way analysis of variance (ANOVA). (B) Graphs summarising flow cytometry data for absolute numbers of CD3+ T cells in salivary glands of WT mice at day 15 pc treated with seletalisib at day 0 (white bars), day 3 (light grey) and day 5 (dark grey) pc as compared with vehicle controls (black bars). Results represented as mean±SD of two independent experiments with five mice; *p<0.05, **p<0.01, ***p<0.001, one-way ANOVA. (C and D) Graphs summarising flow cytometry data for absolute numbers of CD4+ T cells, CD8+ T cells in salivary glands of WT mice at day 15 pc treated with seletalisib at day 0 (white bars), day 3 (light grey) and day 5 (dark grey) pc as compared with vehicle controls (black bars). Results represented as mean±SD of two independent experiments with three mice per group; *p<0.05, **p<0.01, ***p<0.001, one-way ANOVA. (E) Graphs summarising flow cytometry data for absolute numbers of CD19+ B cells in salivary glands of WT mice at day 15 pc treated with seletalisib at day 0 (white bars), day 3 (light grey) and day 5 (dark grey) pc as compared with vehicle controls (black bars). Results represented as mean±SD of two independent experiments with five mice glands per group; *p<0.05, **p<0.01, ***p<0.001, one-way ANOVA. (F–I) Graphs summarising flow cytometry data for absolute numbers of CD19+CD11b−CD5−B2 B cells, follicular (CD23+) B cells and Ki67+ (proliferating) T and B cells in salivary glands of WT mice at day 15 pc treated with seletalisib at day 0 (white bars), day 3 (light grey) and day 5 (dark grey) pc as compared with vehicle controls (black bars). Results represented as mean±SD of two independent experiments with three mice per group; *p<0.05, **p<0.01, ***p<0.001, one-way ANOVA. (J) Graphs summarising flow cytometry data for absolute numbers of B220+ CD138+ plasma cells in salivary glands of WT mice at day 15 pc treated with seletalisib at day 0 (white bars), day 3 (light grey) and day 5 (dark grey) pc as compared with vehicle controls (black bars). Results represented as mean±SD of two independent experiments with five mice per group; **p<0.01, ***p<0.001, one-way ANOVA.

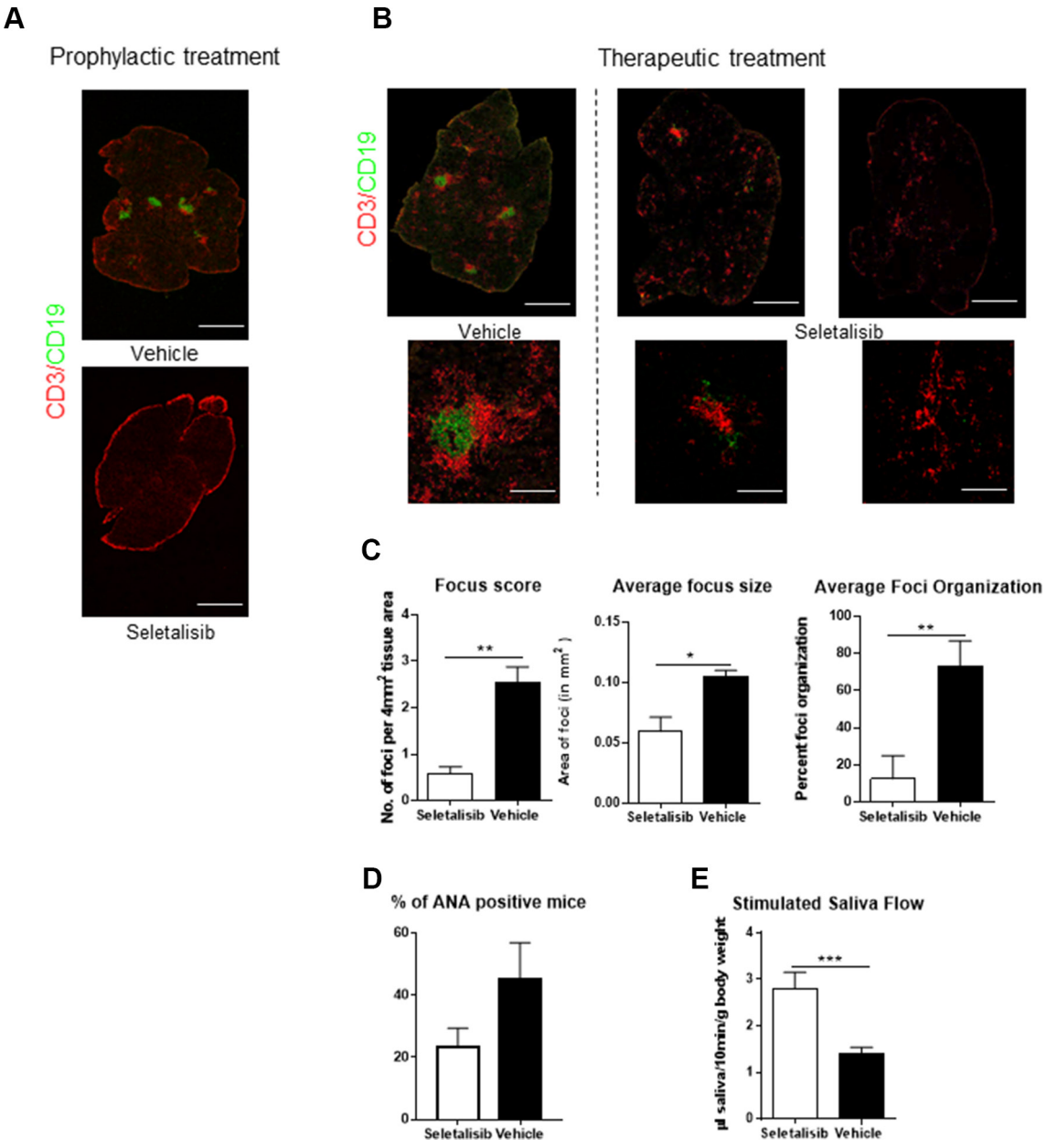

Figure 4 (A and B) Microphotograph of lymphoid aggregates in salivary glands of wild-type (WT) mice at day 15 postcannulation (pc) treated with seletalisib prophylactically or therapeutically as compared with vehicle controls (black bars) stained for CD3 (red) and CD19 (green). Scale bars=500 µm (tile scans) and 100 µm (foci snapshots). (C) Graphs represent the focus score (number of lymphocytic foci (>50 lymphocytes) per 4 mm^2), average size of foci and percentage of segregated aggregates in cannulated salivary glands from therapeutically treated mice as compared with controls. Results represented as mean±SE of two independent experiments with five mice per group; *p<0.05, **p<0.01, ***p<0.001, unpaired t-test. (D) Graphs represent percentage of antinuclear antibodies (ANA) positive mice from seletalisib-treated mice as compared with controls. Results represented as mean±SD of two independent experiments with 10 mice per group, unpaired t-test. (E) Graph comparing salivary flow in seletalisib-treated mice and vehicle controls measured at day 15 pc. Salivary flow is measured as milligrams of saliva produced in 10 min/body weight following pilocarpine stimulation (see the Methods section). Results represented as mean±SD of three independent experiments with 10 mice per group, unpaired t-test.

Interestingly, control lymphoid tissue obtained from mice treated with seletalisib (lymph node and blood) showed minimal impact of the drug on circulating B cells and in the lymph node on the CD4/CD8 ratio (online supplementary figure 6). The anatomical structure of the secondary lymphoid organs was fully conserved in these animals (data not shown).

DISCUSSION

Here, we provide evidence that the PI3Kδ pathway is active and functional in pSS and its blockade in vivo interferes with local and systemic disease progression in an animal model of focal sialoadenitis.

Aberrant B cell activation is the hallmark of pSS. B cell number rises in the SGs during disease progression, correlating with a higher FSC, higher autoantibody titres and the presence of systemic manifestations.[10 19 22 35 36] The increased risk of lymphoma development also correlates with the progressive aggregation of B cells within the SGs and, while a positive association between lymphoma development and GC formation has not been established, the negative

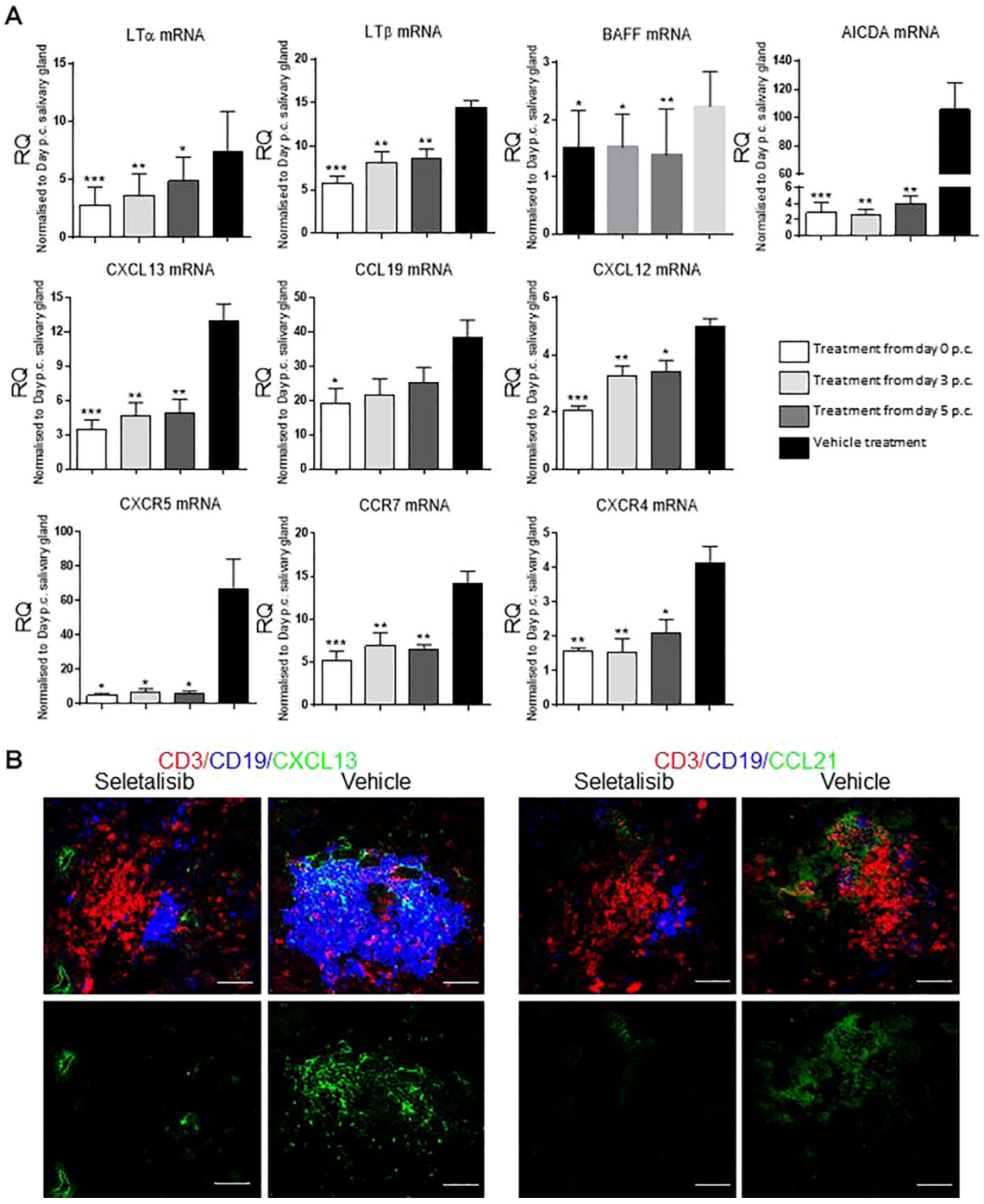

Figure 5 (A) Quantitative real-time-PCR analysis of ltα, ltβ, cxcl13, ccl19, cxcl12, cxcr5, ccr7,cxcr4, baff and aicda mRNA transcripts in salivary glands of wild-type mice at day 15 postcannulation (pc) treated with seletalisib at day 0 (white bars), day 3 (light grey) and day 5 (dark grey) pc as compared with vehicle controls (black bars). Results represented as mean±SD of two independent experiments with five mice per group; *p<0.05, **p<0.01, ***p<0.001, one-way analysis of variance (ANOVA). (B) Microphotograph showing CXCL13 and CCL21 protein expression (green) in day 15 ADV5-infected salivary glands from seletalisib-treated mice as compared with vehicle. T cells (CD3 red) and B cells (CD19 green) are also shown. Scale bars=20 µm.

predictive value of the absence of GC in lymphomagenesis seems clear.[13 17 22 37] More recently, an increased frequency of transitional B cells and mature naive B cells expressing polyreactive antibodies has been demonstrated in the peripheral blood of patients with pSS, confirming that impaired peripheral B cell tolerance plays a critical role in pSS pathogenesis.[38] Accordingly, we previously demonstrated that altering B cell recruitment by blocking the interleukin (IL)-22 mediated production of CXCL13 reduces the formation of SG aggregates and abrogates production of autoantibodies in a mouse model of pSS.[30]

PI3Kδ regulates key aspects of B cell homeostasis. B cells derived from mice deficient in PI3Kδ activity or wild type B cells treated with the PI3Kδ inhibitor all display reduced proliferative ability and increased susceptibility to apoptosis in response to anti-CD40, IL-4 or anti-IgM stimulation.[39 40] Moreover, both B cell response to the BAFF[41] and to the chemoattractant CXCL13 and shingosine-1-phosphate

(S1P) largely relies on PI3Kδ via activation of Rap1, a key GTPase in B lymphocyte migration.[42 43] Memory T cell generation and function is also impaired in the absence of PI3Kδ[6]; thus, unsurprisingly, T cell-dependent antibody responses are also affected in the absence of PI3Kδ isoform.[44] Finally, PI3Kδ-deficient lymphocytes are unable to form polarised synapses efficiently.[44 45]

While the rationale for PI3Kδ targeting in B cell driven autoimmune condition is clear, target validation has not been reported for pSS. Here we demonstrate that the PI3Kδ pathway is activated in pSS and clearly differentiates pSS samples from control sialoadenitis. Expression of the PI3Kδ transcript correlates with manifestations of B cell hyperactivity, including autoantibody production, formation of GCs and hyperglobulinaemia. The expression of pS6, a downstream adaptor of the PI3Kδ pathway, was anticipated in T and B lymphocytes but this marker was also detected in myeloid cells and plasma cells. This finding suggests that patients with pSS and in particular those manifesting B cell symptoms and those characterised by a 'plasma cell signature'[46] have an increased engagement of the PI3Kδ pathway and would benefit from a treatment targeting its activation.

We used a small molecule seletalisib (UCB Celltech), previously demonstrated to be safe and efficacious in patients with psoriasis,[27 47] to target this pathway in vivo, in a model of inducible sialoadenitis.[26] Treatment of cannulated mice with seletalisib resulted in downregulation of S6 phosphorylation and decreased conversion of PIP2 in PIP3, demonstrating the ability of seletalisib to inhibit PI3Kδ activation in treated samples. PI3Kδ blockade in the SGs of our murine model resulted in significantly decreased lymphocyte infiltration, both in terms of T and B cells, disrupted lymphocyte organisation, reduction in autoantibody production, abrogated transcription of lymphoid chemokines and cytokines and improvement in saliva production. In peripheral organs, we observed a non-significant decreased on total cellularity and some changes in the T/B cell ratio and CD4/CD8 ratio. In the blood, we observed a more profound effect on cellularity, probably due to bioavailability and a decrease in total B cell number. Importantly and in agreement with previous publications in human,[27 47] including a recent study in pSS,[48] the mice did not show any sign of infection or unexplained weight loss.

It has been previously demonstrated by us and others that lymphocytes, and in particular T cells, imprint the local microenvironment by releasing LTα, β and proinflammatory cytokines, such as IL-22 or IL-17 that, in turn, regulate the expression of lymphoid chemokines and survival factors necessary for ectopic lymphocyte homing and maintenance in the tissue.[30 49–58] Here we establish that inhibition of PI3Kδ, in seletalisib-treated mice, affects both T and B cells, directly interfering with the establishment of the pathogenic SG microenvironment, preventing the formation of the GC and the perpetuation of local disease.[10 29 30 59–62] These data are in line with previous reports highlighting the role of PI3Kδ in the differentiation of T cells into T helper cells, required for effective GC responses and antibody production.[45 63 64] Accordingly, in our model, abrogation of tissue pathology was accompanied by decreased autoantibody production.

While the effect on antigen presentation and B cell function have been largely described[4 45] and hereby confirmed by the decrease in IL-23 and DC number in the SGs, blood and lymph node, our data highlight a clear requirement for this pathway on plasma cells in our model. In patients with pSS, the aberrant levels of autoantibodies and immunoglobulin are used as biomarkers for disease activity and prognosis.[20 21] GC in the SGs are able to support B cell affinity maturation; moreover, Ro+ and La+ plasma cells have been demonstrated at the periphery of large intraglandular foci. The detection of long-lived CD138+ Bcl-2+ plasma cells in pSS SG has also been associated with higher FSCs,[60 65] more severe systemic manifestation and increased lymphoma risk,[23 66–69] thus establishing that in pSS, local and systemic activation of the plasma cell compartment is involved in disease progression. Here, we demonstrate intense pS6 staining within SG infiltrating plasma cells, suggesting that even on activation, plasma cells are reliant on the PI3Kδ pathway for homeostatic maintenance. Accordingly, in vivo treatment with seletalisib significantly affects plasma cell numbers and abrogates autoantibody production in murine sialoadenitis. Similar data on the efficacy of a PI3Kδ blocking agent have been reported in a phase 2 study, showing a decrease in immunoglobulins in pSS-treated patients as compared with placebo. While primary endpoints were not met in this first study, effects on plasma cells and safety profile from this study support the continued investigation of PI3Kδ inhibitors such as seletalisib in pSS.[48]

All together, these data and the significant correlation between PI3Kδ expression in the glands and clinical manifestations associated with B cell hyperactivation strongly support the evaluation of seletalisib in patients characterised by systemic manifestations, including high levels of immunoglobulins, presence of GCs and high FSC in the biopsies, often identifiable with high levels of ESSDAI.[70–75]

In pSS, B cell-depleting agents, such as rituximab, failed to demonstrate significant clinical success in phase 3 randomised clinical trials, and disease relapse has been observed in patients with pSS (and lymphoma) treated with rituximab.[76–78] While these disappointing findings with rituxumab might in part be due to trial design and choice of outcome measure, biologically, there is evidence of expansion of pathogenic B cell clones following depletion, allegedly supported by the persistent production of survival and chemotactic factors in the SG microenvironment.[77 79–84] Of note, rituximab is unable to target long-lived plasma cells (CD20 negative) directly, thus leaving the autoantibody producing reservoir intact.[85] Consequently, a strategy that aims to target plasma cells directly, alongside T and B lymphocytes, using an agent such as seletalisib, would be desirable in patients with pSS presenting a clear plasma cell signature.[46] Our findings, confirm that in pSS, PI3Kδ has a pleotropic effect on the homeostasis of T, B lymphocytes (including GC B cells) and plasma cells. Selective targeting of PI3Kδ using seletalisib significantly impacts pathogenic microenvironment in the inflamed murine glands, while affecting, systemically, the production of autoantibodies. Overall, these results appear to confirm a mechanistic role for PI3Kδ activity in the immunopathogenesis of pSS supporting the presence and engagement of this pathway in patients characterised by local and systemic B cell hyperactivity. Overall, these results appear to confirm a mechanistic role for PI3Kδ activity in the immunopathogenesis of pSS supporting the presence and engagement of this pathway in human pSS salivary gland and warranting the further evaluation of seletalisib in clinical trials in patients with pSS.

Author affiliations
[1]Centre for Translational Inflammation Research, Institute of Inflammation and Ageing, College of Medical & Dental Sciences, University of Birmingham, Research Laboratories, Queen Elizabeth Hospital, Birmingham, UK
[2]Dipartimento di Medicina Interna e Specialita' Mediche, Sapienza, University of Rome, Rome, Italy
[3]Rheumatology Department, University Hospitals Birmingham NHS Foundation Trust, Birmingham, UK

[4]Department of Rheumatology, Immunology and Allergology, University Hospital, University of Bern, Bern, Switzerland
[5]Immunology, HBRC, University of Birmingham, Birmingham, UK
[6]NIHR Birmingham Biomedical Research Centre, University Hospitals Birmingham NHS Foundation Trust and University of Birmingham, Sandwell and West Birmingham NHS Foundation Trust & Institute of Inflammation and Ageing, University of Birmingham, Birmingham, UK
[7]UCB Pharma, Slough, UK

Contributors SN designed the experimental approach, performed the experiments, analysed the data and wrote the manuscript, JC, CGS, VI, KHH, CB,SC, EP and DHG provided experimental data and contributed to the writing of the manuscript. BAF and FK provided support in analysing human data. RP and GV provided patient material and data, CDB, SJB, MJ and WAF contributed to writing the manuscript. AP and RAA contributed to study design. FB designed the study, analysed the data and wrote the manuscript.

Funding Research funded by UCB Pharma.

Competing interests SN, Grant/Research support: UCB Pharma; RAA, WAF, AP Employee of UCB Pharma. FB, Grant/Research support, ARUK.

Patient consent Obtained.

Ethics approval Ethics number 10-018; Harmonics ethics for the Sapienza, Roma Cohort.

Provenance and peer review Not commissioned; externally peer reviewed.

REFERENCES

1 Vanhaesebroeck B, Whitehead MA, Piñeiro R. Molecules in medicine mini-review: isoforms of PI3K in biology and disease. *J Mol Med* 2016;94:5–11.
2 Baracho GV, Miletic AV, Omori SA, *et al*. Emergence of the PI3-kinase pathway as a central modulator of normal and aberrant B cell differentiation. *Curr Opin Immunol* 2011;23:178–83.
3 Limon JJ, Fruman DA. Akt and mTOR in B cell activation and differentiation. *Front Immunol* 2012;3:228.
4 Okkenhaug K. Signaling by the phosphoinositide 3-kinase family in immune cells. *Annu Rev Immunol* 2013;31:675–704.
5 Lannutti BJ, Meadows SA, Herman SE, *et al*. CAL-101, a p110delta selective phosphatidylinositol-3-kinase inhibitor for the treatment of B-cell malignancies, inhibits PI3K signaling and cellular viability. *Blood* 2011;117:591–4.
6 Soond DR, Bjørgo E, Moltu K, *et al*. PI3K p110delta regulates T-cell cytokine production during primary and secondary immune responses in mice and humans. *Blood* 2010;115:2203–13.
7 Fruman DA, Cantley LC. Idelalisib--a PI3Kδ inhibitor for B-cell cancers. *N Engl J Med* 2014;370:1061–2.
8 Okkenhaug K, Burger JA. PI3K signaling in normal B cells and chronic lymphocytic leukemia (CLL). *Curr Top Microbiol Immunol* 2016;393:123–42.
9 Herman SE, Gordon AL, Wagner AJ, *et al*. Phosphatidylinositol 3-kinase-δ inhibitor CAL-101 shows promising preclinical activity in chronic lymphocytic leukemia by antagonizing intrinsic and extrinsic cellular survival signals. *Blood* 2010;116:2078–88.
10 Barone F, Bombardieri M, Manzo A, *et al*. Association of CXCL13 and CCL21 expression with the progressive organization of lymphoid-like structures in Sjögren's syndrome. *Arthritis Rheum* 2005;52:1773–84.
11 Salomonsson S, Jonsson MV, Skarstein K, *et al*. Cellular basis of ectopic germinal center formation and autoantibody production in the target organ of patients with Sjögren's syndrome. *Arthritis Rheum* 2003;48:3187–201.
12 Bombardieri M, Barone F, Humby F, *et al*. Activation-induced cytidine deaminase expression in follicular dendritic cell networks and interfollicular large B cells supports functionality of ectopic lymphoid neogenesis in autoimmune sialoadenitis and MALT lymphoma in Sjögren's syndrome. *J Immunol* 2007;179:4929–38.
13 Dong L, Chen Y, Masaki Y, *et al*. Possible mechanisms of lymphoma development in Sjögren's syndrome. *Curr Immunol Rev* 2013;9:13–22.
14 Fragkioudaki S, Mavragani CP, Moutsopoulos HM. Predicting the risk for lymphoma development in Sjogren syndrome: an easy tool for clinical use. *Medicine* 2016;95:e3766.
15 Papageorgiou A, Ziogas DC, Mavragani CP, *et al*. Predicting the outcome of Sjogren's syndrome-associated non-hodgkin's lymphoma patients. *PLoS One* 2015;10:e0116189.
16 Johnsen SJ, Brun JG, Gøransson LG, *et al*. Risk of non-Hodgkin's lymphoma in primary Sjögren's syndrome: a population-based study. *Arthritis Care Res* 2013;65:816–21.
17 Theander E, Vasaitis L, Baecklund E, *et al*. Lymphoid organisation in labial salivary gland biopsies is a possible predictor for the development of malignant lymphoma in primary Sjögren's syndrome. *Ann Rheum Dis* 2011;70:1363–8.
18 Giannouli S, Voulgarelis M. Predicting progression to lymphoma in Sjögren's syndrome patients. *Expert Rev Clin Immunol* 2014;10:501–12.
19 Dinescu ŞC, Forţofoiu MC, Bumbea AM, *et al*. Histopathological and immunohistochemical profile in primary Sjögren's syndrome. *Rom J Morphol Embryol* 2017;58:409–17.
20 Tincani A, Andreoli L, Cavazzana I, *et al*. Novel aspects of Sjögren's syndrome in 2012. *BMC Med* 2013;11:93.
21 Brito-Zerón P, Baldini C, Bootsma H, *et al*. Sjögren syndrome. *Nat Rev Dis Primers* 2016;2:16047.
22 Campos J, Hillen MR, Barone F. Salivary gland pathology in Sjögren's syndrome. *Rheum Dis Clin North Am* 2016;42:473–83.
23 Salomonsson S, Wahren-Herlenius M. Local production of Ro/SSA and La/SSB autoantibodies in the target organ coincides with high levels of circulating antibodies in sera of patients with Sjögren's syndrome. *Scand J Rheumatol* 2003;32:79–82.
24 Stefanski AL, Tomiak C, Pleyer U, *et al*. The diagnosis and treatment of Sjögren's syndrome. *Dtsch Arztebl Int* 2017;114:354–61.
25 Ramos-Casals M, Tzioufas AG, Font J. Primary Sjögren's syndrome: new clinical and therapeutic concepts. *Ann Rheum Dis* 2005;64:347–54.
26 Bombardieri M, Barone F, Lucchesi D, *et al*. Inducible tertiary lymphoid structures, autoimmunity, and exocrine dysfunction in a novel model of salivary gland inflammation in C57BL/6 mice. *J Immunol* 2012;189:3767–76.
27 Allen RA, Brookings DC, Powell MJ, *et al*. Seletalisib: characterization of a novel, potent, and selective inhibitor of PI3Kδ. *J Pharmacol Exp Ther* 2017;361:429–40.
28 Vitali C, Bombardieri S, Jonsson R, *et al*. Classification criteria for Sjögren's syndrome: a revised version of the European criteria proposed by the American-European Consensus Group. *Ann Rheum Dis* 2002;61:554–8.
29 Barone F, Bombardieri M, Rosado MM, *et al*. CXCL13, CCL21, and CXCL12 expression in salivary glands of patients with Sjogren's syndrome and MALT lymphoma: association with reactive and malignant areas of lymphoid organization. *J Immunol* 2008;180:5130–40.
30 Barone F, Nayar S, Campos J, *et al*. IL-22 regulates lymphoid chemokine production and assembly of tertiary lymphoid organs. *Proc Natl Acad Sci U S A* 2015;112:11024–9.
31 Nayar S, Campos J, Steinthal N, *et al*. Tissue digestion for stromal cell and leukocyte isolation. *Methods Mol Biol* 2017;1591:225–34.
32 Xu W, He B, Chiu A, *et al*. Epithelial cells trigger frontline immunoglobulin class switching through a pathway regulated by the inhibitor SLPI. *Nat Immunol* 2007;8:294–303.
33 Clark J, Anderson KE, Juvin V, *et al*. Quantification of PtdInsP3 molecular species in cells and tissues by mass spectrometry. *Nat Methods* 2011;8:267–72.
34 Yager N, Haddadeen C, Powell M, *et al*. Expression of PI3K signaling associated with T cells in psoriasis is inhibited by seletalisib, a PI3Kδ inhibitor, and Is required for functional activity. *J Invest Dermatol* 2018;138:1435–9.
35 Aqrawi LA, Skarstein K, Øijordsbakken G, *et al*. Ro52- and Ro60-specific B cell pattern in the salivary glands of patients with primary Sjögren's syndrome. *Clin Exp Immunol* 2013;172:228–37.
36 Voulgarelis M, Tzioufas AG. current aspects of pathogenesis in Sjögren's syndrome. *Ther Adv Musculoskelet Dis* 2010;2:325–34.
37 Barone F, Campos J, Bowman S, *et al*. The value of histopathological examination of salivary gland biopsies in diagnosis, prognosis and treatment of Sjögren's Syndrome. *Swiss Med Wkly* 2015;145:w14168.
38 Glauzy S, Sng J, Bannock JM, *et al*. Defective early B cell tolerance checkpoints in sjögren's syndrome patients. *Arthritis Rheumatol* 2017;69:2203–8.
39 Okkenhaug K, Bilancio A, Farjot G, *et al*. Impaired B and T cell antigen receptor signaling in p110delta PI 3-kinase mutant mice. *Science* 2002;297:1031–4.
40 Bilancio A, Okkenhaug K, Camps M, *et al*. Key role of the p110delta isoform of PI3K in B-cell antigen and IL-4 receptor signaling: comparative analysis of genetic and pharmacologic interference with p110delta function in B cells. *Blood* 2006;107:642–50.
41 Henley T, Kovesdi D, Turner M. B-cell responses to B-cell activation factor of the TNF family (BAFF) are impaired in the absence of PI3K delta. *Eur J Immunol* 2008;38:3543–8.
42 Durand CA, Hartvigsen K, Fogelstrand L, *et al*. Phosphoinositide 3-kinase p110 delta regulates natural antibody production, marginal zone and B-1 B cell function, and autoantibody responses. *J Immunol* 2009;183:5673–84.
43 Reif K, Okkenhaug K, Sasaki T, *et al*. Cutting edge: differential roles for phosphoinositide 3-kinases, p110gamma and p110delta, in lymphocyte chemotaxis and homing. *J Immunol* 2004;173:2236–40.
44 Al-Alwan MM, Okkenhaug K, Vanhaesebroeck B, *et al*. Requirement for phosphoinositide 3-kinase p110delta signaling in B cell antigen receptor-mediated antigen presentation. *J Immunol* 2007;178:2328–35.
45 Hawkins PT, Stephens LR. PI3K signalling in inflammation. *Biochim Biophys Acta* 2015;1851:882–97.

46 Mingueneau M, Boudaoud S, Haskett S, *et al*. Cytometry by time-of-flight immunophenotyping identifies a blood Sjögren's signature correlating with disease activity and glandular inflammation. *J Allergy Clin Immunol* 2016;137:1809–21.
47 Helmer E, Watling M, Jones E, *et al*. First-in-human studies of seletalisib, an orally bioavailable small-molecule PI3Kδ inhibitor for the treatment of immune and inflammatory diseases. *Eur J Clin Pharmacol* 2017;73:581–91.
48 Dörner T, Zeher M, Laessing U. OP0250 A randomised, double-blind study to assess the safety, tolerability and preliminary efficacy of leniolisib (CDZ173) in patients with primary sjÖgren's syndrome. *Annals of the Rheumatic Diseases* 2018;77:174–74.
49 Ansel KM, Ngo VN, Hyman PL, *et al*. A chemokine-driven positive feedback loop organizes lymphoid follicles. *Nature* 2000;406:309–14.
50 Barone F, Gardner DH, Nayar S, *et al*. Stromal fibroblasts in tertiary lymphoid structures: a novel target in chronic inflammation. *Front Immunol* 2016;7:477.
51 Carragher DM, Rangel-Moreno J, Randall TD. Ectopic lymphoid tissues and local immunity. *Semin Immunol* 2008;20:26–42.
52 Cyster JG, Ansel KM, Reif K, *et al*. Follicular stromal cells and lymphocyte homing to follicles. *Immunol Rev* 2000;176:181–93.
53 Kang S, Fedoriw Y, Brenneman EK, *et al*. BAFF induces tertiary lymphoid structures and positions T cells within the glomeruli during lupus nephritis. *J Immunol* 2017;198:2602–11.
54 Ngo VN, Korner H, Gunn MD, *et al*. Lymphotoxin alpha/beta and tumor necrosis factor are required for stromal cell expression of homing chemokines in B and T cell areas of the spleen. *J Exp Med* 1999;189:403–12.
55 Schneider K, Potter KG, Ware CF. Lymphotoxin and LIGHT signaling pathways and target genes. *Immunol Rev* 2004;202:49–66.
56 Tumanov A, Kuprash D, Lagarkova M, *et al*. Distinct role of surface lymphotoxin expressed by B cells in the organization of secondary lymphoid tissues. *Immunity* 2002;17:239–50.
57 Tumanov AV, Kuprash DV, Mach JA, *et al*. Lymphotoxin and TNF produced by B cells are dispensable for maintenance of the follicle-associated epithelium but are required for development of lymphoid follicles in the Peyer's patches. *J Immunol* 2004;173:86–91.
58 Tumanov AV, Kuprash DV, Nedospasov SA. The role of lymphotoxin in development and maintenance of secondary lymphoid tissues. *Cytokine Growth Factor Rev* 2003;14:275–88.
59 Liu Z, Davidson A. BAFF and selection of autoreactive B cells. *Trends Immunol* 2011;32:388–94.
60 Szyszko EA, Brokstad KA, Oijordsbakken G, *et al*. Salivary glands of primary Sjögren's syndrome patients express factors vital for plasma cell survival. *Arthritis Res Ther* 2011;13:R2.
61 Groom J, Kalled SL, Cutler AH, *et al*. Association of BAFF/BLyS overexpression and altered B cell differentiation with Sjögren's syndrome. *J Clin Invest* 2002;109:59–68.
62 Jonsson MV, Szodoray P, Jellestad S, *et al*. Association between circulating levels of the novel TNF family members APRIL and BAFF and lymphoid organization in primary Sjögren's syndrome. *J Clin Immunol* 2005;25:189–201.
63 Rolf J, Bell SE, Kovesdi D, *et al*. Phosphoinositide 3-kinase activity in T cells regulates the magnitude of the germinal center reaction. *J Immunol* 2010;185:4042–52.
64 Venable JD, Ameriks MK, Blevitt JM, *et al*. Phosphoinositide 3-kinase gamma (PI3Kgamma) inhibitors for the treatment of inflammation and autoimmune disease. *Recent Pat Inflamm Allergy Drug Discov* 2010;4:1–15.
65 Szyszko EA, Brun JG, Skarstein K, *et al*. Phenotypic diversity of peripheral blood plasma cells in primary Sjögren's syndrome. *Scand J Immunol* 2011;73:18–28.
66 Sutcliffe N, Inanc M, Speight P, *et al*. Predictors of lymphoma development in primary Sjögren's syndrome. *Semin Arthritis Rheum* 1998;28:80–7.
67 Voulgarelis M, Dafni UG, Isenberg DA, *et al*. Malignant lymphoma in primary Sjögren's syndrome: a multicenter, retrospective, clinical study by the European Concerted Action on Sjögren's Syndrome. *Arthritis Rheum* 1999;42:1765–72.
68 Tengnér P, Halse AK, Haga HJ, *et al*. Detection of anti-Ro/SSA and anti-La/SSB autoantibody-producing cells in salivary glands from patients with Sjögren's syndrome. *Arthritis Rheum* 1998;41:2238–48.
69 Theander E, Henriksson G, Ljungberg O, *et al*. Lymphoma and other malignancies in primary Sjögren's syndrome: a cohort study on cancer incidence and lymphoma predictors. *Ann Rheum Dis* 2006;65:796–803.
70 Seror R, Ravaud P, Bowman SJ, *et al*. EULAR Sjogren's syndrome disease activity index: development of a consensus systemic disease activity index for primary Sjogren's syndrome. *Ann Rheum Dis* 2010;69:1103–9.
71 ter Borg EJ, Risselada AP, Kelder JC. Relation of systemic autoantibodies to the number of extraglandular manifestations in primary Sjögren's Syndrome: a retrospective analysis of 65 patients in the Netherlands. *Semin Arthritis Rheum* 2011;40:547–51.
72 Gottenberg JE, Seror R, Miceli-Richard C, *et al*. Serum levels of beta2-microglobulin and free light chains of immunoglobulins are associated with systemic disease activity in primary Sjögren's syndrome. Data at enrollment in the prospective ASSESS cohort. *PLoS One* 2013;8:e59868.
73 Ramos-Casals M, Brito-Zerón P, Seror R, *et al*. Characterization of systemic disease in primary Sjögren's syndrome: EULAR-SS Task Force recommendations for articular, cutaneous, pulmonary and renal involvements. *Rheumatology* 2015;54:2230–8.
74 Risselada AP, Hair M, Kruize AA, *et al*. Lymphocytic focus score as a prognostic tool. *Ann Rheum Dis* 2015;74:e31.
75 Devauchelle-Pensec V, Gottenberg JE, Jousse-Joulin S, *et al*. which and how many patients should be included in randomised controlled trials to demonstrate the efficacy of biologics in primary sjögren's syndrome? *PLoS One* 2015;10:e0133907.
76 St Clair EW, Levesque MC, Prak ET, *et al*. Rituximab therapy for primary Sjögren's syndrome: an open-label clinical trial and mechanistic analysis. *Arthritis Rheum* 2013;65:1097–106.
77 Quartuccio L, Fabris M, Moretti M, *et al*. Resistance to rituximab therapy and local BAFF overexpression in Sjögren's syndrome-related myoepithelial sialadenitis and low-grade parotid B-cell lymphoma. *Open Rheumatol J* 2008;2:38–43.
78 Saraux A, Pers JO, Devauchelle-Pensec V. Treatment of primary Sjögren syndrome. *Nat Rev Rheumatol* 2016;12:456–71.
79 Cornec D, Costa S, Devauchelle-Pensec V, *et al*. Blood and salivary-gland BAFF-driven B-cell hyperactivity is associated to rituximab inefficacy in primary Sjögren's syndrome. *J Autoimmun* 2016;67:102–10.
80 Pers JO, Devauchelle V, Daridon C, *et al*. BAFF-modulated repopulation of B lymphocytes in the blood and salivary glands of rituximab-treated patients with Sjögren's syndrome. *Arthritis Rheum* 2007;56:1464–77.
81 Pers JO, Daridon C, Bendaoud B, *et al*. B-cell depletion and repopulation in autoimmune diseases. *Clin Rev Allergy Immunol* 2008;34:50–5.
82 Quartuccio L, Fabris M, Salvin S, *et al*. Controversies on rituximab therapy in sjögren syndrome-associated lymphoproliferation. *Int J Rheumatol* 2009;2009:1–8.
83 Vos K, Thurlings RM, Wijbrandts CA, *et al*. Early effects of rituximab on the synovial cell infiltrate in patients with rheumatoid arthritis. *Arthritis Rheum* 2007;56:772–8.
84 Boumans MJ, Thurlings RM, Gerlag DM, *et al*. Response to rituximab in patients with rheumatoid arthritis in different compartments of the immune system. *Arthritis Rheum* 2011;63:3187–94.
85 Hamza N, Bootsma H, Yuvaraj S, *et al*. Persistence of immunoglobulin-producing cells in parotid salivary glands of patients with primary Sjögren's syndrome after B cell depletion therapy. *Ann Rheum Dis* 2012;71:1881–7.